Strategic design of a multifunctional urea-triphenylamine benzotriazole-based material

Carlos Tardío[1], Esther Pinilla-Peñalver[2], Beatriz Donoso[3], Basanta Saikia[4], Pablo Fernández[1], Iván Torres-Moya[5]*

[1]Department of Inorganic, Organic Chemistry and Biochemistry, Faculty of Chemical Science and Technologies, Instituto Regional de Investigación Científica Aplicada (IRICA), University of Castilla-La Mancha, 13071 Ciudad Real, Spain.

[2]Department of Analytical Chemistry and Food Technology, University of Castilla-La Mancha, Avenue Camilo José Cela, s/n, 13071 Ciudad Real, Spain.

[3]Department of Organic Chemistry, Faculty of Sciences, Campus of Fuentenueva, University of Granada, 18071 Granada, Spain.

[4]Department of Chemistry, Molecular Imaging and Photonics, KULAK—KU Leuven, E. Sabbelaan 53, 8500 Kortrijk, Belgium.

[5]Department of Organic Chemistry, Faculty of Chemical Sciences, Campus of Espinardo, University of Murcia, 30010 Murcia, Spain.

Correspondence: ivan.torres@um.es

Abstract

The search for multifunctional derivatives is of paramount importance in material science considering sustainability, practicality, and applicability. For this reason, this article presents a multifunctional benzotriazole derivative synthesized through rational design, showcasing its versatility across diverse applications. The tailored functionality of the compound enables it to serve in photonics as an optical waveguide, as smart material as stimuli responsiveness material, and as a gelator for drug crystallization in pharmaceuticals. This work underscores the power of rational design for organic synthesis in creating versatile materials with broad applicability.

Introduction

In today's society, characterized by a growing demand for innovative and sustainable solutions, the quest for multifunctional materials holds a central place in scientific and technological research. Materials science plays a pivotal role in offering new materials

with diverse properties and functionalities that can address contemporary challenges in areas such as energy, health, environment, and technology. In this context, the search for multifunctional materials has become a primary goal for researchers in materials science. These materials have the potential to optimize resource usage, reduce environmental footprint, and enhance the efficiency of a wide range of industrial and everyday applications. Furthermore, the ability to integrate multiple functions into a single material can lead to significant advancements in areas such as personalized medicine, flexible electronics, energy storage and conversion, among others [1-3]. Consequently, the development and characterization of multifunctional materials represent an exciting and promising field in pursuing innovative solutions to contemporary challenges.

Organic molecules can be used to achieve multifunctional materials due to their interesting characteristics when compared to their inorganic counterparts. They are lighter, display diverse morphologies, and importantly, their characteristics can be finely adjusted at the molecular level through the opportunities provided by organic synthesis [4-6].

Among the plethora of organic compounds, the benzotriazole core (BTZ), distinguished by its heterocyclic bicyclic structure, stands out for its exceptional properties, rendering it a remarkably versatile constituent in material engineering. Functioning as a moderate electron acceptor moiety owing to its polarizable imine unit (C=N), its chemical framework provides a sturdy foundation for electronic conjugation, facilitating precise adjustment of the optical and electronic attributes of associated materials. The incorporation of the triazole functional group not only confers chemical stability but also promotes the formation of conjugated bonds, thereby augmenting charge transfer efficiency. Moreover, the benzotriazole's capacity to modulate the HOMO-LUMO energy levels, attributed to the labile N-H bond in the benzotriazole moiety, allowing to introduce alkynyl or aryl derivatives and the facile introduction of various electroattractor or electrodonor groups at positions 4 and 7 of the benzene ring [7,8].

For all these reasons, BTZ could be a very versatile moiety to design multifunctional materials. In pursuit of the objective of design a multifunctional derivative with different applications, a meticulous and systematic design of compound **1** was undertaken to ensure that each molecular fragment contributes the desired characteristics. To this end, BTZ was selected as the acceptor core for all the reasons previously described. In our case, we have

focused our attention on designing a multifunctional material with optical waveguiding behaviour, stimuli responsiveness and as a gelator for drug crystallization.

As depicted in Figure 1, the BTZ core has been functionalized at the 4,7-position with an alkynyl triphenylamine group (TPA), because this group can offer intense fluorescence, desirable for optical waveguiding behaviour, contributing also to red-shifting and interesting for stimuli responsiveness materials [9,10]. BTZ and TPA are linked with an alkynyl group, which favours the formation of supramolecular structures because of its ability to generate C-H···π interactions, phenomena previously observed by our research group [11,12]. However, the combination of BTZ and TPA increases the rigidity of the aromatic system. For this reason, we have functionalized the BTZ core with a long alkyl chain to increase the solubility and flexibility and we have taken advantage of this fact by adding a urea function in the alkyl chain to increase the possibility of gelation processes because it is well-known that hydrogen bonds in urea groups can induce gel formation [13-14].

With this functionalization, we hope that our derivative can exhibit multifunctional characteristics and be successful in the applications that we want.

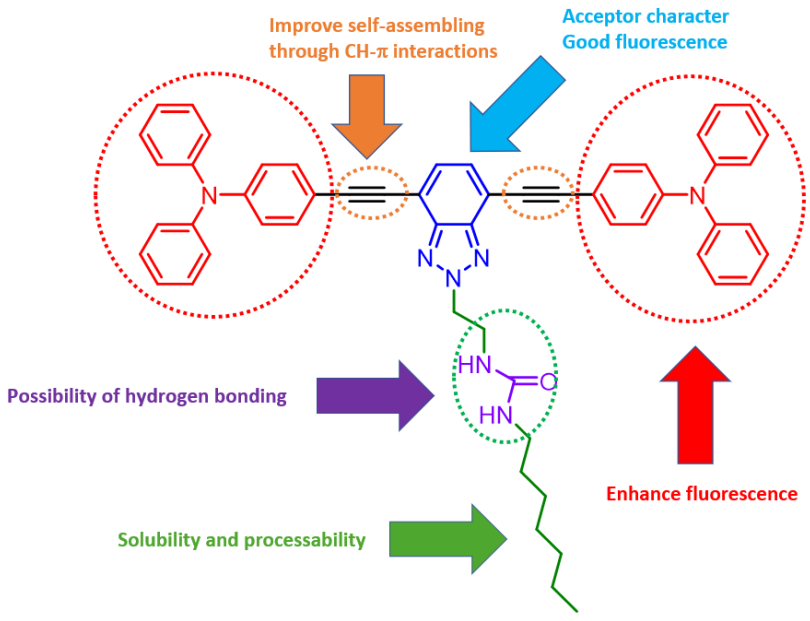

Figure 1. Rational design of BTZ-based derivative **1** with the different functionalities that can provide each fragment of the designed multifunctional compound.

Results and discussion

Synthesis

The synthesis of the desired derivative **1** was started by a N-alkylation of BTZ core with the N-ureaBoc derivative of N-(2-bromoethyl)-N'-dodecylurea (N-BocDDU) employing potassium tert-butoxide as base in methanol, and then deprotecting the Boc group with trifluoroacetic acid. It can be pointed out that NH groups of the urea group were firstly protected with the Boc group to avoid deprotonation and competition in the N-alkylation of the BTZ core. The bromination of the benzotriazole **3** followed the synthetic route to achieve the dibromobenzotriazole **4** [15]. Finally, a Sonogashira C-C cross-coupling reaction between the dibromobenzotriazole **4** and the alkynyl fragment of triphenylamine was performed (Scheme 1). The reaction was carried out under microwave irradiation using reusablePd-EncatTPP30. This design and synthesis is a more environmentally friendly procedure, as previously optimized by our research group for other benzoazoles [16].

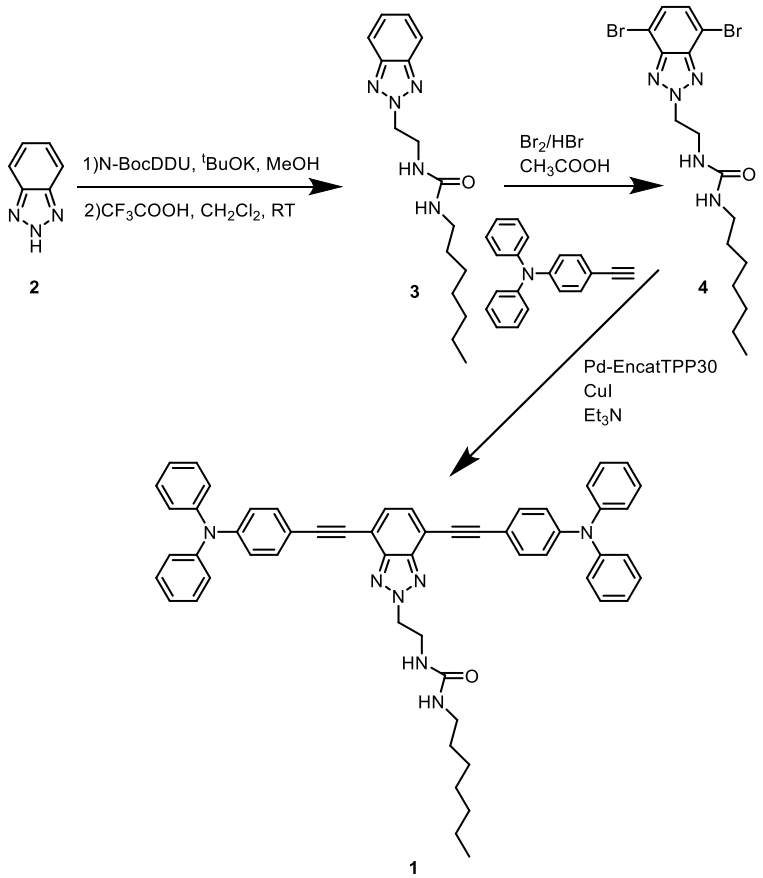

Scheme **1**. Synthetic procedure of the desired derivative **1**, object of study in this work.

Photophysical data

The UV-vis and fluorescence spectra of the derivative **1** were carried out in 10^{-5} M CH_2Cl_2 solutions. They are shown in Figure 2 and photophysical data are summarized in Table 1.

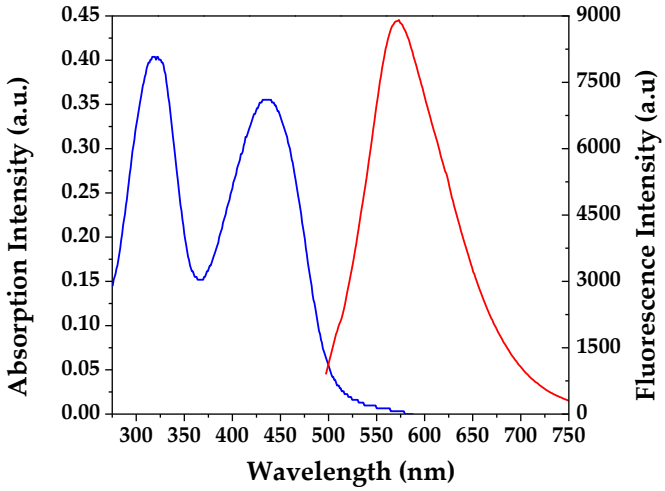

Figure 2. Absorption (blue) and emission (red) spectra of derivative **1** in 10^{-5}M CH_2Cl_2 solutions.

Table 1. Photophysical data of derivative **1**.

Compound	**λ_{abs}[a] (nm)**	**λ_{em}[b](nm)**	**λ_{emsol}[c] (nm)**	**λ_{onset} [d] (nm)**	**Φ[e]**	**HOMO-LUMO gap[f] (eV)**	**HOMO-LUMO gap[g] (eV)**
1	326, 431	573	596	515	0.55	2.50	2.41

[a] Maxima of absorption bands of derivative **1** in solution; [b] Maxima of emission bands of derivative **1** in solution; [c] Maxima of emission bands of crystals of derivative **1**; [d] Onset wavelength calculated from the absorption spectra; [e] PL Quantum yield of derivative **1.** [f] Theoretical HOMO-LUMO gap of derivative **1** calculated at B3LYP/6-31G(d,p) level. [g] Experimental HOMO-LUMO gap of derivative **1** calculated from the onset of the lowest energy absorptions.

Derivative **1** exhibited absorption spectra characterized by a broad band with a peak centered at 326 nm, attributed to a π- π* transition, and a second band centered at a longer wavelength (431 nm), attributed to an intramolecular charge transfer (ICT) state. When

the photoluminescence (PL) spectra were obtained following photoexcitation at the peak of the longest-wavelength absorption band, the maxima shift was centered at 573 nm.

The experimental optical HOMO-LUMO gap was determined based on the onset of the lowest energy band absorption and demonstrated satisfactory agreement with theoretical calculations (Table 1). Notably, a redshift in PL is observed in the solid state, compared to the solution phase (573 vs 596 nm).

Finally, the fluorescence quantum yield of derivative **1** in solution (fluorescence orange solution) was determined in CH_2Cl_2 employing quinine sulfate in 0.1 M H_2SO_4 ($\Phi = 0.54$) and fluorescein in 0.1 M NaOH ($\Phi = 0.79$) as reference standards, showing a good value of 0.55 (Table 1).

BTZ 1 as optical waveguide

Optical waveguides have emerged as a crucial component in the advancement of modern technologies due to their ability to transmit light with high efficiency and minimal loss. In the telecommunications field, these structures are fundamental for data transmission through optical fibers, which form the backbone of high-speed internet networks. Waveguides can handle large volumes of data at lightning-fast speeds, essential for the functioning of the digital economy and connected society. Additionally, in the realm of photonic devices, waveguides are key elements in the development of photonic integrated circuits, enabling the miniaturization and performance enhancement of components such as lasers, modulators, and optical detectors. These innovations not only increase the efficiency and capacity of communication systems but also drive advances in areas such as quantum computing and lidar technology for autonomous vehicles [17-20].

In this sense, BTZ **1** could be powerful for this application because the possibility of self-assembling and good fluorescence that it shows. To evaluate the capability of **1** as an optical waveguide, the material is subjected to crystallization to obtain good-quality crystals. The slow diffusion technique was used for the crystallization. Then, in a glass vial, 1 mg of the compound was dissolved in 1 mL of tetrahydrofuran or chloroform. The vial was gently placed into a second vial containing 4 mL of a solvent in which the compound is not soluble, such as ethanol, methanol, or hexane. Needle-shaped crystals were obtained after 3-4 days.

The crystals showed well-defined surfaces, lengths ranging from tens to hundreds μm and thicknesses ranging from 4 to 30 μm. Moreover, interestingly SEM images of the crystals

revealed the existence of many crystals interconnected to each other forming cross-linked structures (Figure 3).

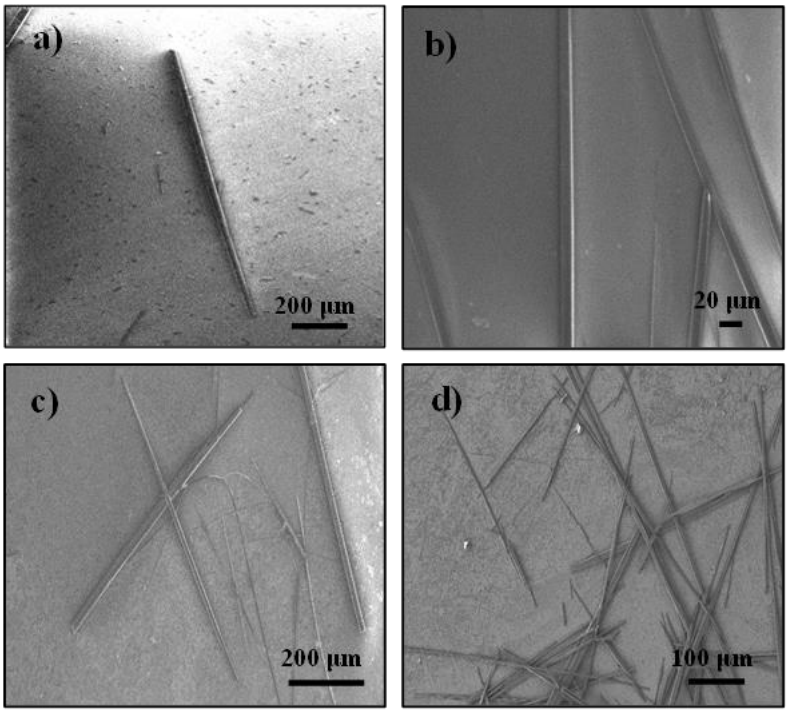

Figure 3. SEM images of the supramolecular aggregates of **1** in THF/MeOH.

Unfortunately, despite several attempts, the crystals do not give enough diffraction to obtain a single crystal structure. However, based on our experience with this type of D-A-D compounds [21,22], it is very likely that the structure is governed by hydrogen bonds involving the -NH of the urea groups, as well as by C-H···π interactions involving the triple bonds.

To probe the optical waveguide propensity of the crystals, a single rod of length, L ≈ 500 µm, was excited at the left corner with a 365 nm laser. As a result, a bright orange fluorescence (FL) was generated at the excitation point, as well as at the right corner of the crystals, because of the FL transduced through its long axis from the excitation point to the emission point. This result confirmed the active optical waveguiding capability of BTZ **1** (Figure 4).

The FL at the emission point showed a maximum of 596 nm. Notably, the solid-state emission band exhibited a bathochromic shift compared to the solution (Table 1). This shift was caused by the higher dielectric constant of the solid medium and the presence of intermolecular interactions [23].

Likewise, given the waveguiding nature of the structures and the existence of naturally interconnected linear crystals, we explored the possibility of creating photonic circuits. For that, we identified a network forming a nearly *Y*-shaped junction. The circuit was composed of two crystals (Figure 4). The length of the longest crystal was 600 μm, whereas the shorter arm had a length of 250 μm. The junction points of both crystals consisted of the end of the shorter crystal and the interior of the longer crystal, specifically about 200 μm from its left end. Thus, the circuit was composed of three outputs (1-3) and a junction (J1).

After excitation at point J1, FL emission was observed at each of the circuit's output points (1-3). It is important to note that the emission intensity at point 3 was lower than that observed at points 1 and 2, possibly due to the longer propagation distance. Nevertheless, the ability to transmit light to different emission points simultaneously and in any direction was confirmed. This characteristic holds significant value in integrated circuits as it enables detection by other devices simultaneously [24].

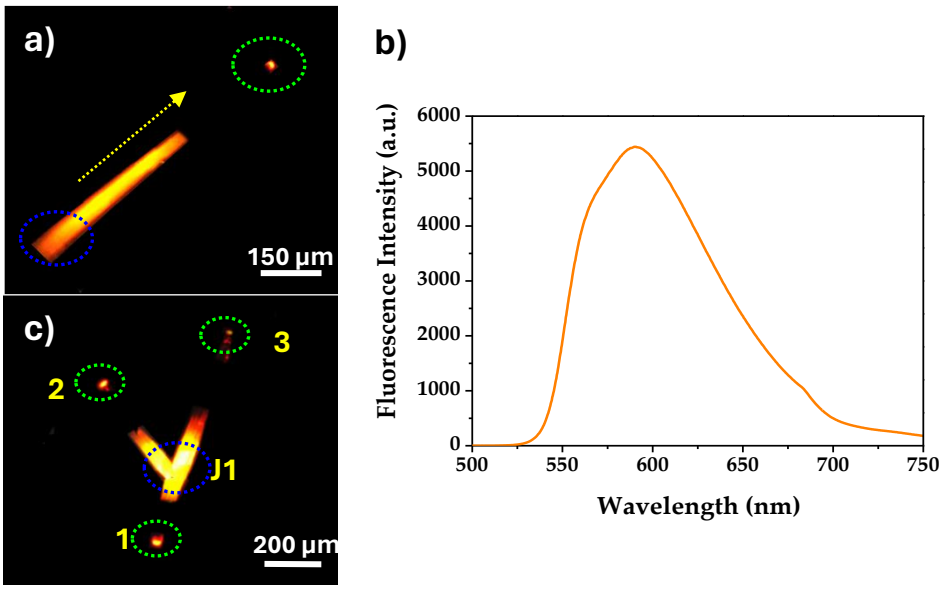

Figure 4. a) FL image of crystal of **1**. b) PL spectra of fiber of **1.** c) FL image of the junction excited at J1. Blue circle denotes excitation points, green circles denote emission points, and the arrow denotes the light propagation direction.

BTZ 1 as Stimuli-responsiveness material

The integration of optical waveguiding properties and stimuli responsiveness within a singular material garners significant interest for potential applications in optoelectronics

and sensor domains. For instance, Yawen et al. detailed five cyanofunctionalized 1,4-bis((E)-2-(1H-indol-3-yl)vinyl)benzene derivatives, substituted with alkyl chains of varying lengths [25]. Remarkably, while compounds with shorter side chains exhibited optical waveguiding properties, those with longer chains displayed thermochromism. In another instance, Jia et al. reported a singular organic crystal of a derivative linking a pyrene unit and a rhodamine B moiety through a CN group. This crystal demonstrated multifaceted properties including optical waveguiding and mechanochromism [26]. In addition, we can find in the literature some examples of triphenylamine derivatives with stimuli responsiveness [9, 27-29].

Motivated by all these previous results, we were aimed to study stimuli responsiveness for derivative **1**. In this specific case, we have detected that the emission properties in the solid state of derivative **1** can be tuned in response to changes in the temperature. Indeed, the fluorescence properties of thin films prepared by spin-coating of derivative **1** (with thicknesses of around 300 nm) changed notably when they were heated at 100ºC, as it is noticed in Figure 5a in which we can observe the emission of the thin film visualized under a UV lamp (λ=365 nm) before the annealing at 100ºC and after that showing the heat-induced colour change from orange to yellow. After that, the primitive emission colour can be recovered in the films by simply grinding with a spatula. Fluorescence spectra of the emissive films of **1** after thermal treatment confirmed that in PL spectrum showed a blue-shift from 560 nm to 518 nm (Figure 5b), and revealed that, upon later shearing after the previous annealing the emission wavelength is recovered, returning to the initial point. This fact makes this derivative interesting for possible temperature sensing applications. It can be pointed out that the absorption spectra of the films before and after heating do not change.

The π···π stacking is a prerequisite for photochemical reaction. A plausible explanation is that when heated, a more crystalline phase is obtained, and the initial amorphous phase is recovered after shearing. The material might show colour polymorphism, however, this phenomenon is out of the scope of the present work. The blue-shift could be explained because some conjugated derivatives with potential aggregation like derivative **1**, because of the hydrogen bonding and CH-π interactions, possess the ability to form excimers with associative interactions between ground and excites state molecules, which can explain that the a priori, the unexpected red-shifted in amorphous phases [30,31].

(a) (b)

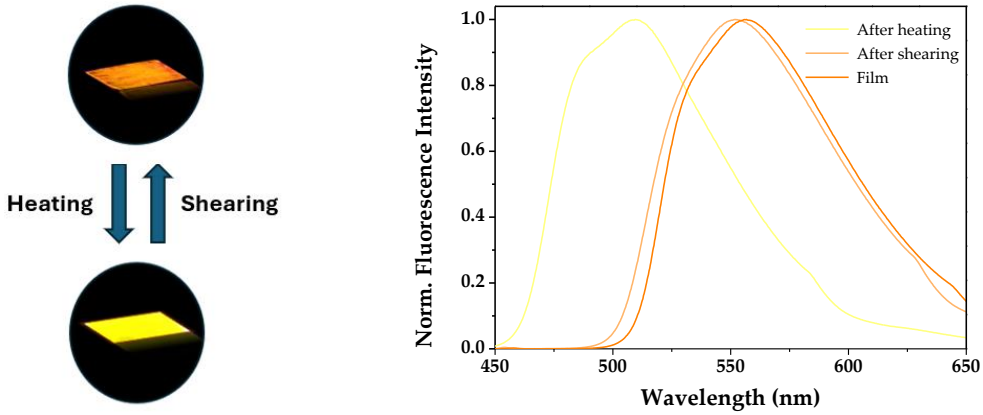

Figure 5. (a) Photos of thin films of derivative **1** illuminated under a 365 nm lamp after heating and shearing. (b) Fluorescence spectra of the thin films of derivative **1**, obtained by spin-coating, after heating and later shearing to recover the initial colour.

BTZ 1 as a gelator for drug crystallization

In recent years, gels have gained increasing importance in the field of materials science due to their unique properties and versatility in various applications. These materials, which can exhibit both liquid and solid characteristics, possess a three-dimensional network that endows them with capabilities such as retaining large amounts of liquid, flexibility, and a remarkable responsiveness to external stimuli. Advances in the understanding and manipulation of gels have enabled their use in diverse areas such as medicine, where hydrogels are employed in controlled drug delivery and tissue engineering; in technology, where aerogels are valued for their exceptional thermal and acoustic insulating properties; and in the food industry, where gels contribute to the creation of new products with enhanced textures and properties [32-36]. Ongoing research in this field is opening up new possibilities for the design of smart and sustainable materials, highlighting the importance of gels as a fundamental tool in contemporary technological and scientific innovation.

One of the most relevant applications in the last years is the drug crystallization, essential in the pharmaceutical industry [37-39]. The introduction of the NH groups in the alkyl chain of BTZ **1** were purposely introduced in order to explore this application.

First of all, gelation experiments were conducted for derivative **1** using almost thirty different solvents at various concentrations (2% wt, 1% wt, and 0.5% wt). The gelators were dissolved in 0.5 mL of the chosen solvent through gentle heating, followed by sonication for 1 minute until fully dissolved. The vials were then left undisturbed at room temperature. The flow properties of the resulting mixtures were assessed using the simple tube inversion test, with observations made at 4, 24, 48, and 72 hours. The outcomes showed that derivative **1** gave some gels at a concentration of 2%wt in alcoholic solvents like 1-propanol, 1-butanol, 1,4-butanediol or ethylene glycol. At 1%wt and 0.5%wt no gels were observed.

The different gels were characterized exploring thermal stability (T_{sol}) by the dropping ball method and mechanical resistance (yield stress) by rheology experiments (see Supporting Information). Critical gelation concentration (CGCs) for all the solvents were also calculated. In general, no significant differences were observed between the gels in terms of thermal stability, being the gel in ethylene glycol the most thermally stable and the 1-butanol the less one (Table S2). However, gel in 1-propanol is much more mechanically resistant with a yield stress of 985, in comparison that the gel in 1-butanol that can be broken easily (see Table S3 and Figure S3).

Then, aimed by the good thermal and mechanical stability of the gels, specially in 1-propanol, organogels obtained from 1-propanol of **1** were examined as powerful crystallization media for some APIs. Different representative APIs were selected for these studies based on their known polymorphism, chemical diversity and some mimicry because they all possess NH groups that can form hydrogen bonds between the gelator and the drug: theophylline, sulfathiazole, sulfamerazine and flufenamic acid (Figure S4).

For these studies, some crystallization experiments were conducted to optimize the crystallization conditions. For gelation, it was found that a drug concentration of 5 mg/mL with a gelator concentration of 2% was effective for our purpose. The gelator and drug were mixed in a specific solvent, heated gently, and then sonicated to form a gel of the API solution. The samples in open vials were then left undisturbed at room temperature for several weeks to allow for crystallization. In many instances, crystallization did not occur. The experiments were repeated three times with the same results in all the cases to verify the reproducibility. The vials were checked visually for crystallization and crystalline products analysed by X-ray powder and single crystal diffraction.

No significant difference on crystallization outcome between gel and a solution phase control experiment under the same conditions, was observed in the cases of theophylline, sulfamerazine and flufenamic acid in terms of morphology and polymorphic form. The experiments resulted in the known Form II in the case of theophylline [40], the Pna21 polymorph in the case of sulfamerazine [41] and form IV in the case of flufenamic acid [42]. In the gel phase crystallization of sulfathiazole some changes were observed. In terms of morphology, in general, smaller crystals in terms of length but wider in terms of width were observed and in addition a change from polymorphic Form II in solution to room temperature kinetic Form I was observed in the presence of the gel (Figure 6) [43]. Quantitative characterization of the polymorphs obtained by unit cell determination supports this fact (Figure S5). This interesting outcome suggests that the gels from derivative **1** either inhibits crystallization of Form II or increases the nucleation rate of Form I. These gels obtained by gelation of gelator **1** present significant potential for broadening the range of current polymorph discovery methods, particularly within the pharmaceutical industry.

(a) (b)

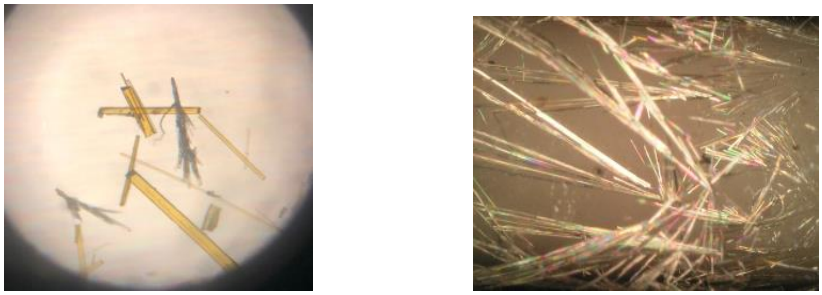

Figure 6. Crystals of sulfathiazole grown in 1-propanol gels of **1** (a) and by solution evaporation (b).

Experimental section

General techniques

All the chemicals employed for the synthesis of derivative **1** were procured commercially. Reactions involving air-sensitive materials were conducted under an atmosphere of argon. Microwave irradiations were executed using a Discover® (CEM, Matthews, NC, USA). focused microwave reactor. Silica gel, (Merck, Kieselgel 60, 230–240 mesh, Merck, Darmstadt, Germany), was employed for flash chromatography. Analytical thin layer

chromatography (TLC) was carried out on aluminium-coated Merck Kieselgel 60 F254 plates (Merck, Darmstadt, Germany).

^{1}H-NMR and ^{13}C-NMR spectra collection were recorded using a Bruker Advance Neo NMR spectrometer that operates at 300 MHz for ^{1}H and 75 MHz for ^{13}C. All spectra were acquired at 298 K, employing partially deuterated solvents as internal references. Coupling constants (J) are expressed in hertz (Hz), and chemical shifts (δ) are reported in parts per million (ppm). Multiplicities are described in the following way: s = singlet, d = doublet, t = triplet, m = multiplet.

For elemental analysis experiments (EA) C, H, N and S micro-sample elemental analyzer LECO (model CNHS-932, St. Joseph, MI, USA) was used, employing 2 mg of sample for each experiment.

Mass spectra were obtained on a Bruker Autoflex II TOF/TOF (Bruker, Billerica, MA, USA) spectrometer using dithranol as the matrix for all the experiments.

The thin films were prepared by chloroform solutions of **1** that were spin-coated at 1500 rpm/s of rotational acceleration, using a spin coater Laurell Technologies WS-650MX-23NPP.

UV–visible and fluorescence spectra studies in solution were carried out using a Jasco V-750 spectrophotometer (JASCO-Spain, Madrid, Spain) and Jasco FP-8300 spectrofluorimeter (JASCO-Spain, Madrid, Spain), respectively. The absorption and emission spectra were taken using dichloromethane as a solvent and at a concentration of 10^{-5} M at room temperature using standard quartz cells of 1 cm width and high spectroscopic grade solvents with very high purity.

PL microscopy images of crystals were captured using a Nikon Eclipse Ti inverted microscope with dry objectives (100X N.A. 0.8 and 20X N.A. 0.45). This setup was coupled to a Shamrock spectrometer from Andor Technology, equipped with a thermoelectrically cooled Newton EM (Andor) CCD. The excitation was achieved by appropriately filtering the lines from a Xe lamp.

Conclusions

This work demonstrates a design-based approach to synthesize a multifunctional benzotriazole organic material via precise functionalization. This approach has proven

highly effective in developing a material with versatile and promising applications in various technological and scientific fields.

Controlled synthesis and appropriate functionalization have allowed us to obtain a material with remarkable optical properties and optical waveguiding behaviour, responsiveness to stimuli, and utility as a gel for drug crystallization. These characteristics position it as an ideal candidate for applications in photonics devices, smart sensors, and the pharmaceutical industry.

This study highlights the potential of chemical synthesis and molecular engineering to design materials with specific and versatile applications. Furthermore, it underscores the importance of interdisciplinary research in seeking innovative solutions to current technological and scientific challenges.

Experimental data

Synthesis of 1-(2-(4,7-bis((4-(diphenylamino)phenyl)ethynyl)-2H-benzo[d][1,2,3]triazol-2-yl)ethyl)-3-heptylurea (**1**): A mixture of 1-(2-(4,7-dibromo-2H-benzo[d][1,2,3]triazol-2-yl)ethyl)-3-heptylurea (**4**) (0.100 g, 0.139 mmol), 4-ethynyl-N,N-diphenylaniline (**5**) (0.082 g, 0.306 mmol), DBU (0.046 g, 0.306 mmol), CuI (0.001 g, $6.95x10^{-3}$ mmol) and Pd- EncatTM TPP30 (0.027 g, 0.014 mmol) was charged to a dried microwave vessel under an argon atmosphere. After that, 1 mL of CH_3CN was added to the vessel, which next was closed and was irradiated at 130ºC for 20 min. The crude reaction was purified by column chromatography, employing hexane/ethyl acetate 1:1 as eluent to get analytically pure the desired product **1** as a dark orange solid (0.055 g, 47%).

^{1}H-NMR ($CDCl_3$, 300MHz), δ: 7.67 (s, 2H, $H_{benzotriazole}$), 7.45-7.43 (d, 4H, H_{phenyl}), 7.26-7.23 (t, 8H, H_{phenyl}), 7.16-7.15 (dd, 8H, H_{phenyl}), 7.08-7.07 (d, 4H, H_{phenyl}), 6.96-6.93 (tt, 4H, H_{phenyl}), 5.71 (s, 1H, NH), 5.35 (s, 1H, NH), 4.51-4.49 (t, 2H, -CH_2), 3.52-3.50 (dd, 2H, -CH_2), 3.09-3.00 (dt, 2H, -CH_2), 1.56-1.53 (m, 2H, -CH_2), 1.42-1.40 (m, 2H, -CH_2), 1.33-1.26 (m, 6H, -CH_2), 1.02-0.99 (t, 3H, -CH_3). ^{13}C-NMR ($CDCl_3$, 75MHz), δ:159.1, 148.9, 145.6, 145.4, 131.4, 129.8, 128.3, 126.3, 125.8, 124.9, 119.7, 108.5, 91.9, 75.6, 49.0, 40.4, 31.6, 31.2, 29.5, 29.1, 27.4, 22.9, 14.0. MS (EI): m/z: 838,87 [M+]. EA; Calculated for $C_{56}H_{51}N_7O$; C: 80.26; H: 6.13; N: 11.70, found C: 80.37; H: 6.18; N: 11.58.

Acknowledgments

I. Torres-Moya is indebted by Juan de la Cierva Formación 2020 FJC2020-043684-I with assistance financed by MCIN/AEI/10.13039/501100011033 and for the Unión Europea Next Generation EU/PRTR. University of Castilla-La Mancha was also acknowledged.

Authorship contribution

Carlos Tardío: Investigation, Discussion, Writing- original draft, preparation. **Esther Pinilla-Peñalver**: Investigation, Discussion. **Beatriz Donoso**: Investigation, Discussion. **Basanta Saikia**: Investigation, Discussion. **Pablo Fernández**: Investigation. **Iván Torres Moya**: Conceptualization, Investigation, Discussion, Supervision, Writing – review & editing.

References

[1] Abdelhamid HN. An introductory review on advanced multifunctional materials. Heliyon 2023;9:e18060. https://doi.org/10.1016/j.heliyon.2023.e18060.

[2] Huang Y, Wang X. Challenges and Trends for Multifunctional Materials. Jour of Build Mater Sci 2023;5:17–9. https://doi.org/10.30564/jbms.v5i1.5521.

[3] Ferreira ADBL, Nóvoa PRO, Marques AT. Multifunctional material systems: A state-of-the-art review. Compos Struct 2016;151:3–35. https://doi.org/10.1016/j.compstruct.2016.01.028.

[4] Yao Y, Dong H, Hu W. Charge transport in organic and polymeric semiconductors for flexible and stretchable devices. Adv Mater 2016;28:4513–23. https://doi.org/10.1002/adma.201503007.

[5] Neto BAD, Carvalho PHPR, Correa JR. Benzothiadiazole derivatives as fluorescence imaging probes: Beyond classical scaffolds. Acc Chem Res 2015;48:1560–9. https://doi.org/10.1021/ar500468p.

[6] Beaujuge PM, Fréchet JMJ. Molecular design and ordering effects in π-functional materials for transistor and solar cell applications. J Am Chem Soc 2011;133:20009–29. https://doi.org/10.1021/ja2073643.

[7] Balan A, Baran D, Toppare L. Benzotriazole containing conjugated polymers for multipurpose organic electronic applications. Polym Chem 2011;2:1029–43. https://doi.org/10.1039/c1py00007a.

[8] Balan A, Gunbas G, Durmus A, Toppare L. Donor−Acceptor polymer with benzotriazole moiety: Enhancing the electrochromic properties of the “donor unit.” Chem Mater 2008;20:7510–3. https://doi.org/10.1021/cm802937x.

[9] Hariharan PS, Prasad VK, Nandi S, Anoop A, Moon D, Anthony SP. Molecular engineering of triphenylamine based aggregation enhanced emissive fluorophore: Structure-dependent mechanochromism and self-reversible fluorescence switching. Cryst Growth Des 2017;17:146–55. https://doi.org/10.1021/acs.cgd.6b01363.

[10] Yuan WZ, Gong Y, Chen S, Shen XY, Lam JWY, Lu P, et al. Efficient solid emitters with aggregation-induced emission and intramolecular charge transfer characteristics: Molecular design, synthesis, photophysical behaviors, and OLED application. Chem Mater 2012;24:1518–28. https://doi.org/10.1021/cm300416y.

[11] Pastor MJ, Torres I, Cebrián C, Carrillo JR, Díaz-Ortiz Á, Matesanz E, et al. 4-aryl-3,5-bis(arylethynyl)aryl-4H-1,2,4-triazoles: Multitasking skeleton as a self-assembling unit. Chemistry 2015;21:1795–802. https://doi.org/10.1002/chem.201404243.

[12] Torres I, Carrillo JR, Díaz-Ortiz A, Martín R, Gómez MV, Stegemann L, et al. Self-assembly of T-shape 2H-benzo[d][1,2,3]-triazoles. Optical waveguide and photophysical properties. RSC Adv 2016;6:36544–53. https://doi.org/10.1039/c6ra02473d.

[13] Schön E-M, Marqués-López E, Herrera RP, Alemán C, Díaz DD. Exploiting molecular self-assembly: From urea-based organocatalysts to multifunctional supramolecular gels. Chemistry 2014;20:10720–31. https://doi.org/10.1002/chem.201402436.

[14] Peveler WJ, Packman H, Alexander S, Chauhan RR, Hayes LM, Macdonald TJ, et al. A new family of urea-based low molecular-weight organogelators for environmental remediation: the influence of structure. Soft Matter 2018;14:8821–7. https://doi.org/10.1039/c8sm01682h.

[15] Kanik FE, Rende E, Timur S, Toppare L. A novel functional conducting polymer: synthesis and application to biomolecule immobilization. J Mater Chem 2012;22:22517. https://doi.org/10.1039/c2jm34100j.

[16] Torres-Moya I, Carrillo JR, Díaz-Ortiz Á, Prieto P. New Organic Materials Based on Multitask 2H-benzo[d]1,2,3-triazole Moiety. Chemosensors 2021;9:267. https://doi.org/10.3390/chemosensors9090267.

[17] Ravi J, Annadhasan M, Kumar AV, Chandrasekar R. Mechanically reconfigurable organic photonic integrated circuits made from two electronically different flexible microcrystals. Adv Funct Mater 2021;31. https://doi.org/10.1002/adfm.202100642.

[18] Karothu DP, Dushaq G, Ahmed E, Catalano L, Polavaram S, Ferreira R, et al. Mechanically robust amino acid crystals as fiber-optic transducers and wide bandpass filters for optical communication in the near-infrared. Nat Commun 2021;12:1–8. https://doi.org/10.1038/s41467-

[19] Wang C, Zhang D, Yue J, Zhang X, Wu Z, Zhang T, et al. Optical waveguide sensors for measuring human temperature and humidity with gel polymer electrolytes. ACS Appl Mater Interfaces 2021;13:60384–92. https://doi.org/10.1021/acsami.1c13802.

[20] Yu X, Liu B, Pan X, Zhang H. Deep-red-emissive flexible optical waveguide with high elastic performance based on an organic crystal. ChemPhotoChem 2022;6. https://doi.org/10.1002/cptc.202200038.

[21] Tardío C, Álvarez Conde J, Rodríguez AM, Prieto P, Hoz A de la, Cabanillas-González J, et al. Donor–acceptor–donor 1H-Benzo[d]imidazole derivatives as optical waveguides. Molecules 2023;28:4631. https://doi.org/10.3390/molecules28124631.

[22] Vinay Pradeep V, Tardío C, Torres-Moya I, Rodríguez AM, Vinod Kumar A, Annadhasan M, et al. Mechanical processing of naturally bent organic crystalline microoptical waveguides and junctions. Small 2021;17. https://doi.org/10.1002/smll.202006795.

[23] Gierschner J, Cornil J, Egelhaaf H-J. Optical bandgaps of π-conjugated organic materials at the polymer limit: Experiment and theory. Adv Mater 2007;19:173–91. https://doi.org/10.1002/adma.200600277.

[24] Li Z-Z, Tao Y-C, Wang X-D, Liao L-S. Organic nanophotonics: Self-assembled single-crystalline homo-/heterostructures for optical waveguides. ACS Photonics 2018;5:3763–71. https://doi.org/10.1021/acsphotonics.8b00815.

[25] Ma Y, Li Y, Chen L, Xiong Y, Yin G. Cyano-functionalized 1,4-bis((E)-2-(1 H -indol-3-yl)vinyl)benzenes with aggregation induced emission characteristic and diverse thermochromic behaviour. Dyes Pigm 2016;126:194–201. https://doi.org/10.1016/j.dyepig.2015.12.002.

[26] Li Y, Ma Z, Li A, Xu W, Wang Y, Jiang H, et al. A single crystal with multiple functions of optical waveguide, aggregation-induced emission, and mechanochromism. ACS Appl Mater Interfaces 2017;9:8910–8. https://doi.org/10.1021/acsami.7b00195.

[27] Li Z, Ishizuka H, Sei Y, Akita M, Yoshizawa M. Extended fluorochromism of anthracene trimers with a meta-substituted triphenylamine or triphenylphosphine core. Chem Asian J 2012;7:1789–94. https://doi.org/10.1002/asia.201200310.

[28] Gayathri P, Pannipara M, Al-Sehemi AG, Anthony SP. Triphenylamine-based stimuli-responsive solid state fluorescent materials. New J Chem 2020;44:8680–96. https://doi.org/10.1039/d0nj00588f.

[29] Xu L, Huang Y, Peng H, Xu W, Yi X, He G. Triphenylamine-modified cinnamaldehyde derivate as a molecular sensor for viscosity detection in liquids. ACS Omega 2023;8:13213–21. https://doi.org/10.1021/acsomega.3c00488.

[30] Cho DW, Cho DW. Excimer and exciplex emissions of 1,8-naphthalimides caused by aggregation in extremely polar or nonpolar solvents. New J Chem 2014;38:2233–6. https://doi.org/10.1039/c3nj01473h.

[31] Cho DW, Fujitsuka M, Choi KH, Park MJ, Yoon UC, Majima T. Intramolecular exciplex and intermolecular excimer formation of 1,8-Naphthalimide−Linker−Phenothiazine dyads. J Phys Chem B 2006;110:4576–82. https://doi.org/10.1021/jp056078p.

[32] Sheng F, Zhang B, Zhang Y, Li Y, Cheng R, Wei C, et al. Ultrastretchable organogel/silicone fiber-helical sensors for self-powered implantable ligament strain monitoring. ACS Nano 2022;16:10958–67. https://doi.org/10.1021/acsnano.2c03365.

[33] Koo J, Lim S-I, Jang J, Oh M, Jeong K-U. From polymer gels to 3D actuators: Transformation of programmed 2D structures to 3D objects. J Chem Educ 2020;97:1396–401. https://doi.org/10.1021/acs.jchemed.9b01150.

[34] Chaudhary S, Chakraborty E. Hydrogel based tissue engineering and its future applications in personalized disease modeling and regenerative therapy. Beni-Suef Univ J Basic Appl Sci 2022;11. https://doi.org/10.1186/s43088-021-00172-1.

[35] Esposito CL, Kirilov P, Roullin VG. Organogels, promising drug delivery systems: an update of state-of-the-art and recent applications. J Control Release 2018;271:1–20. https://doi.org/10.1016/j.jconrel.2017.12.019.

[36] Zhang XN, Zheng Q, Wu ZL. Recent advances in 3D printing of tough hydrogels: A review. Compos B Eng 2022;238:109895. https://doi.org/10.1016/j.compositesb.2022.109895.

[37] Foster JA, Damodaran KK, Maurin A, Day GM, Thompson HPG, Cameron GJ, et al. Pharmaceutical polymorph control in a drug-mimetic supramolecular gel. Chem Sci 2017;8:78–84. https://doi.org/10.1039/c6sc04126d.

[38] Foster JA, Piepenbrock M-OM, Lloyd GO, Clarke N, Howard JAK, Steed JW. Anion-switchable supramolecular gels for controlling pharmaceutical crystal growth. Nat Chem 2010;2:1037–43. https://doi.org/10.1038/nchem.859.

[39] Aparicio F, Matesanz E, Sánchez L. Cooperative self-assembly of linear organogelators. Amplification of chirality and crystal growth of pharmaceutical ingredients. Chem Commun (Camb) 2012;48:5757. https://doi.org/10.1039/c2cc31818k.

[40] Seton L, Khamar D, Bradshaw IJ, Hutcheon GA. Solid state forms of theophylline: Presenting a new anhydrous polymorph. Cryst Growth Des 2010;10:3879–86. https://doi.org/10.1021/cg100165t.

[41] Pallipurath AR, Skelton JM, Warren MR, Kamali N, McArdle P, Erxleben A. Sulfamerazine: Understanding the influence of slip planes in the polymorphic phase transformation through X-ray crystallographic studies and ab initio lattice dynamics. Mol Pharm 2015;12:3735–48. https://doi.org/10.1021/acs.molpharmaceut.5b00504.

[42] Zhang K, Fellah N, López-Mejías V, Ward MD. Polymorphic phase transformation pathways under nanoconfinement: Flufenamic acid. Cryst Growth Des 2020;20:7098–103. https://doi.org/10.1021/acs.cgd.0c01207.

[43] Munroe Á, Rasmuson ÅC, Hodnett BK, Croker DM. Relative stabilities of the five polymorphs of sulfathiazole. Cryst Growth Des 2012;12:2825–35. https://doi.org/10.1021/cg201641g.